Article

The Accuracy of a Marine Satellite Compass under Terrestrial Urban Conditions

Paweł S. Dąbrowski [1],*[iD], **Cezary Specht** [1][iD], **Andrzej Felski** [2][iD], **Władysław Koc** [3],
Andrzej Wilk [2], **Krzysztof Czaplewski** [1][iD], **Krzysztof Karwowski** [4], **Krzysztof Jaskólski** [2][iD],
Mariusz Specht [5][iD], **Piotr Chrostowski** [3][iD] and **Jacek Szmagliński** [3][iD]

[1] Department of Geodesy and Oceanography, Gdynia Maritime University, 81347 Gdynia, Poland;
c.specht@wn.umg.edu.pl (C.S.); k.czaplewski@wn.umg.edu.pl (K.C.)

[2] Polish Naval Academy, Institute of Navigation and Maritime Hydrography, 81127 Gdynia, Poland;
a.felski@amw.gdynia.pl (A.F.); andrzej.wilk@pg.edu.pl (A.W.); k.jaskolski@amw.gdynia.pl (K.J.)

[3] Faculty of Civil and Environmental Engineering, Gdańsk University of Technology, 80233 Gdańsk, Poland;
kocwl@pg.edu.pl (W.K.); piochros@pg.edu.pl (P.C.); jacszmag@pg.edu.pl (J.S.)

[4] Faculty of Electrical and Control Engineering, Gdańsk University of Technology, 80233 Gdańsk, Poland;
krzysztof.karwowski@pg.edu.pl

[5] Department of Transport and Logistics, Gdynia Maritime University, 81225 Gdynia, Poland;
m.specht@wn.umg.edu.pl

* Correspondence: p.dabrowski@wn.umg.edu.pl; Tel.: +48-58-5586-810

Abstract: When used at sea, satellite compasses are capable of determining the course of a sailing vessel with high accuracy. It is difficult to verify the accuracy declared by the device manufacturer under such conditions, as it is difficult to define a reliable reference. This study analyses the accuracy of the satellite compass in an urban setting, with the satellite signal being obscured to various extents. It is an important point in the study to refer the measurement results to a reference route, which is the axis of a tramway track, determined by the precise GNSS RTK method. The measurement data were processed in the original software developed by the authors. The results demonstrate a high 2D positioning accuracy with low height determination accuracy. The course determination errors exceed the limit values declared by the manufacturer. However, specific measurement conditions must be taken into account, which differ considerably from the typical applications of a satellite compass.

Keywords: satellite compass; accuracy; positioning; course; GPS

1. Introduction

The GPS system plays an extremely important role in marine, land and air navigation. Owing to the nearly full system availability around the globe, a user's position can be determined to an accuracy of several meters [1]. The GPS system consists of three functionally interlinked segments: land-based, control-based and space-based [2]. The GPS system has been modernised continuously since the beginning of its operation with the aim of gradually improving its functions. Such progress has been most noticeable as a change in the satellite constellation [3]. Older satellite blocks have been replaced with newer models equipped with modules that allow for satellite signal transmission on new frequencies [4]. Currently, satellite receivers used for object positioning mostly do not only use the GPS system. The Russian Glonass, Chinese BeiDou and European Galileo systems are also widely used. The number of global navigation satellite systems (GNSS) depends on the class and the intended use of a device. Precise geodetic receivers can usually make use of all GNSS, which is associated with a relatively high price for the measurement apparatus. Now that mobile devices are commonly used for navigation and as maps, their motherboards often contain positioning modules using three GNSS

systems [5]. This study uses a satellite compass based only on the GPS system, which is sufficient given its use at sea. The absence of any features that obscure the sky at sea means that the GNSS receivers can trace a higher number of satellites than at sea than on land.

A marine satellite compass consists of at least two integrated satellite receivers. Owing to simultaneous positioning by both the devices, it is possible to calculate the current course of a vessel. Therefore, together with a magnetic compass, a satellite compass is an additional, independent source of navigation information. The study used a Furuno SC-50 satellite compass, which—according to the producer's declaration—has a Root-Mean-Square (RMS) error of the course determination of 0.5° and a positioning error of 10 m and 5 m with DGPS corrections (level of confidence p = 0.95) [6]. This study aimed at empirical determination of device accuracy in atypical measurement conditions. The experiment was conducted at night on 28/29 November 2018 as part of the measurement work for the InnoSatTrack research project (POIR.04.01.01-00-0017/17) carried out by a consortium of two universities: Gdańsk University of Technology and Gdynia Maritime University. The project examines the possibility of improving the accuracy of geometric parameters of a railway track with a specific number of GNSS satellite receivers. Improvement of the GPS and Glonass system accuracy [7,8], construction of new systems (Galileo/Beidou) and creating new multi-constellation geodetic GNSS systems [9] have contributed to the rapid development of the method. Studies were conducted in 2009–2017 in two main directions: geodetic—associated with increasing the measurement accuracy and availability [10–12], and related to the device construction—aimed at developing new design and operation methods [13–16]. Further examination of the method under development was conducted at Gdańsk Brzeźno on a several-kilometre tramway track with variable sky visibility conditions. Considering the broad range of the GNSS stock-taking measurements of the railway track, measurements were conducted simultaneously with the aim of assessing the performance (accuracy) of the satellite compass operation in non-standard terrain conditions, which were variable with respect to the extent the GNSS signal was obscured.

Researchers from Calgary occupy a significant place in this group, among others [17]. However, similar studies have been conducted in other North American [18,19] and Polish [20] centres. Satellite compasses have been in widespread use for at least a decade, but only few reports on this subject were published, e.g., reference [21,22]. On a tramway passage, receiver positions were recorded, determined with the RTK differential method with centimetre accuracy levels [23]. Therefore, successive point coordinates indicating the course of the tramway track axis provided a reliable reference for synchronous observations registered by the satellite compass. Apart from the measurement procedure, this paper presents the methodology of a mean error determination for the compass position and course. It also emphasises the significant factor of Gauss-Krüger projection and the Polish state coordinate system PL-2000 [24]. The findings will be compared to the accuracy declared by the producer, taking into account specific conditions of the measurement. The first attempts to use several receivers to determine the orientation angles of a moving object were made as early as in the 1990s.

2. Materials and Methods

The measuring instruments used in the experiment were placed on three trolleys of a DWF 300 series tramway (dimensions: 2.73 m × 1.78 m × 0.75 m) and pulled behind a Bombardier tramway [25]. Five GNSS satellite receivers from two producers were installed on each of the two trolleys. Five Leica GS15 receivers were placed in a specific geometric configuration on the middle trolley and five Trimble R10 receivers were placed on the third (last) trolley. The first trolley was fitted out with a steel support with a Furuno SC-50 satellite compass. The central receivers on the last two platforms and the satellite compass were placed above the tramway track axis. A staking out procedure of a Leica TPS 1103

electronic total station was used for their precision deployment. The coordinates of the tachymetric prisms and instruments were determined by the following formulas:

$$\begin{cases} x = d \sin(V) \cos(Hz) \\ y = d \sin(V) \sin(Hz) \\ z = d \cos(V) \end{cases} \tag{1}$$

where:

x, y, z—ortho-Cartesian coordinates of a point,
d—slope distance to a point,
V—vertical angle of the total station target axis,
Hz—horizontal angle of the total station target axis.

This method allowed for precise (with a millimetre-error) determination of the target position of the measurement equipment. The deployment diagram for the equipment used in the experiment is presented in Figure 1.
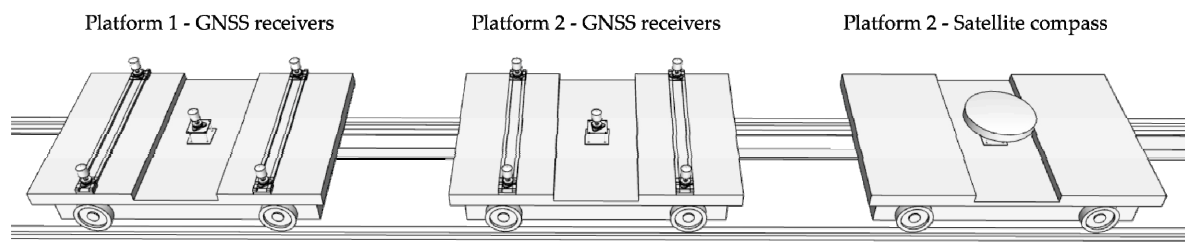
Figure 1. The measuring instruments used in satellite measurements at night on 28 November 2018–29 November 2018.

The tramway and the measurement trolley route ran through an urbanised area in which the sky was obscured to varying extent. The tramway started at the terminus in Gdańsk Brzeźno and went southwards along Józef Haller Avenue. There are no buildings in the vicinity in this section and the conditions for satellite measurements were favourable. At the crossroads, the route turned south-eastwards along Maciej Płażyński Avenue. There were no objects which would obscure the sky here either. The tramway turned north-eastwards at the next crossroads, along Gdańska Street. The sky in this section was partly obscured by roadside trees and buildings. The last part of the planned closed route ran along the westward tramway track section between the entrance to the beach and the tramway terminus. Unlike in the section along Gdańska Street, there were many buildings in the immediate vicinity of the track. The route diagram is shown in Figure 2.

Figure 2. The route of the satellite measurement at night on 28 November 2018–29 November 2018 described in [26].

The tramway covered the planned route over a dozen times, with satellite compass observations recorded at a frequency of 1 Hz during three passages. The satellite receivers on the other two trolleys recorded their positions at a frequency of 20 Hz. This provided a number of measured points on the reference route that was adopted in this study. They were later used for determining the reference values for the satellite compass observations. Figure 3 shows selected stages of the measurements.

Figure 3. Preparations (**a**) and the measuring instruments during the measurement at night on 28 November 2018–29 November 2018 (**b**).

The files with the satellite observations data were transferred from the satellite receivers to an external drive. The compass data were registered in real time on the hard drive of a computer inside the tramway. Measurement data from the satellite compass were saved as text files in the NMEA 0183

format [27]. The data included the following types of NMEA messages: $GPZDA, $GPGGA, $GPGLL, $GPHDT. The $GPZDA contains information on the registration time—the hour (UTC time), date (day, month, year) and the time zone. The $GPGGA type is especially commonly used in general positioning because it can be used to read out the curvilinear coordinates (geodetic longitude and latitude) and to calculate the point coordinates in a selected map projection. A $GPGGA message contains information on the position registration time (UTC), geodetic latitude and longitude, positioning quality (e.g., using DGPS differential systems), number of satellites, the value of the Horizontal Dilution of Precision (HDOP), orthometric height, the distance between the geoid and the ellipsoid interpolated from the model, differential data origin and age data. The $GPGLL type contains selected fields of the previous two types, i.e., geodetic latitude and longitude, and the position registration time. The last type of NMEA message transmitted by a satellite compass is $GPHDT. It contains information on the vehicle current course relative to the northward direction. Table 1 contains a section of data from the NMEA stream.

Table 1. Satellite compass observations in the NMEA format from a selected measurement epoch.

$GPZDA,002507,29,11,2018,00,00*48
$GPGGA,002507,5424.0178,N,01837.6592,E,1,08,1.9,40,M,,M,,*7A
$GPGLL,5424.0178,N,01837.6592,E,002507,A,A*4B
$GPHDT,58.9,T*01

Curvilinear coordinates of geographic latitude and longitude were projected onto a plane to achieve the study objectives. Thus, metric units were obtained which made it possible to calculate the positioning and the course errors. The PL-2000 state coordinate system is used in Poland for map projections for land surveying purposes [18], which was obtained by modification of the Gauss-Krüger cylindrical transverse projection. This projection is obtained by placing the image (cylinder) surface in the transverse direction relative to the Earth's rotation axis. The PL-2000 system embraces four longitudinal zones which are 3° wide, and the axial meridians are 15°, 18°, 21° and 24° of the eastern geodetic longitude [28]. The deployment of the longitudinal zones is shown in Figure 4.
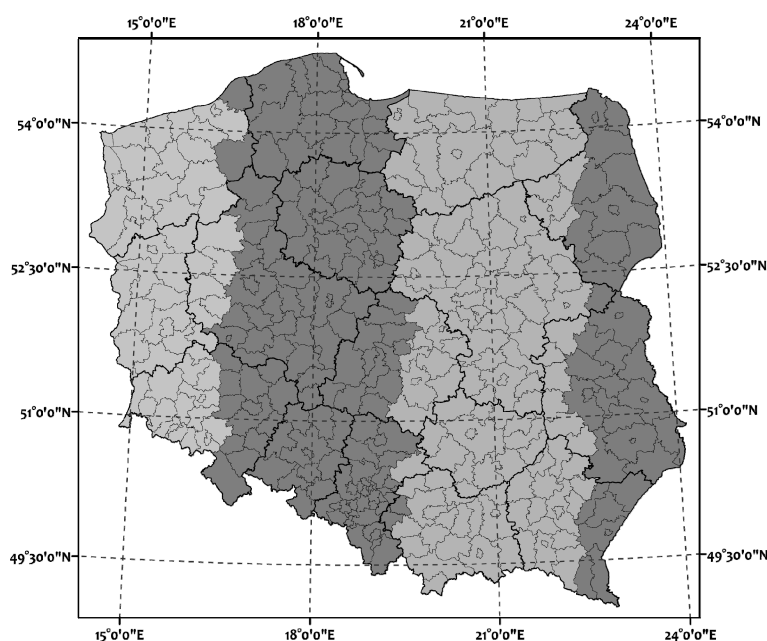
Figure 4. Longitudinal zones of the PL-2000 coordinate system.

The study area is situated in zone 6 of the PL-2000 system with an axial meridian of 18°. Determination of the satellite compass accuracy in variable urban conditions involved calculation of the position and course error relative to the reference value based on the GNSS RTK differential observations of one of the satellite receivers. This solution is justified because, despite determination of the navigation parameters in the same measurement epoch at various points of the railway track axis, it was possible to develop an algorithm which assigned satellite observations of both devices according to the criterion of position. To be more precise, the frequency of 20 Hz of the RTK reference measurements enabled a quality assessment of each observation recorded by the satellite compass to be performed. This solution is presented in Figure 5.
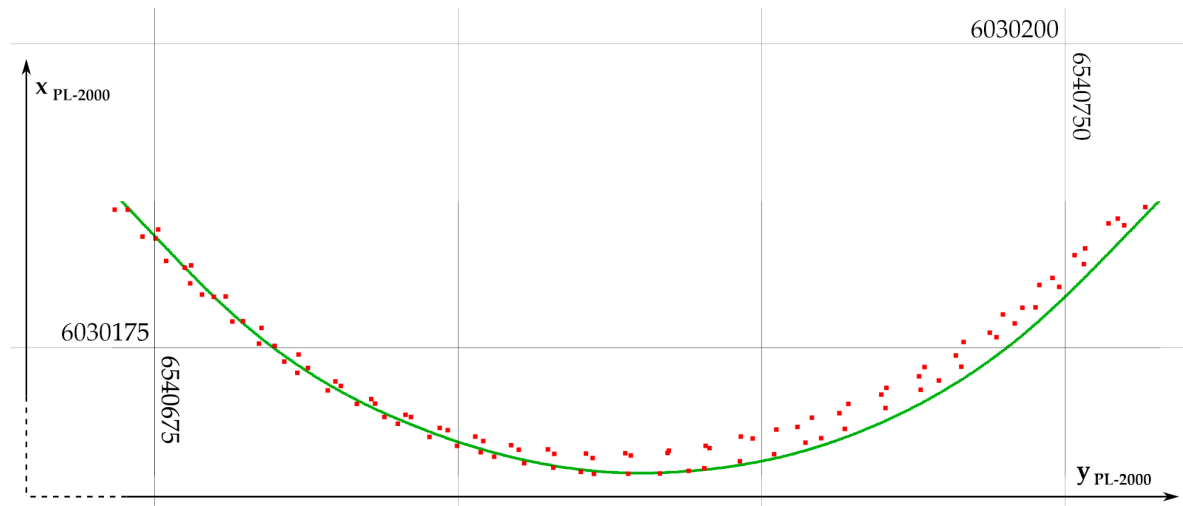
Figure 5. The tramway track position determined by the satellite compass in three test passages along the test route (red, frequency 1 Hz) and an analogous determination of the GNSS satellite receiver in one passage (green, frequency 20 Hz).

An increased frequency of the reference measurement translated to the mean distance of 0.20 m between consecutive determination of the tramway track position at a mean vehicle velocity of 15 km/h. Furthermore, the frequency of the satellite compass measurement of 1 Hz ensured that consecutive observations would be recorded at a linear interval of ca. 4 m. Therefore, with the right methodology, it was possible to select a reliable sample of reference data from the GNSS receiver observation set. The Python language software used two input text files containing selected and processed data from NMEA messages (satellite compass) and the GNSS measurement report (GNSS receiver). The first input file contained satellite compass observations (Table 2).

Table 2. Fragment of the input file containing satellite compass observations.

ID_{pom}	$y_{PL-2000}$ [m]	$x_{PL-2000}$ [m]	H_{Ort} [m]	Measurement Epoch [yyyy, mm, dd, UTC]	Latitude [°]	Longitude [°]	H_{Ort} [m]	SVs [−]	HDOP [−]	HDG_1 [°]	HDG_2 [°]
1	6537589.012	6029098.277	61	2018, 11, 28, 22:59:27	54.390735	18.578695	61	5	4.6	326.2	326.1
2	6537589.647	6029100.138	61	2018, 11, 28, 22:59:28	54.39075167	18.578705	61	6	2.6	326.1	326.1
3	6537590.391	6029101.814	61	2018, 11, 28,22:59:29	54.39076667	18.57871667	61	7	2.5	326	326
4	6537591.135	6029103.49	62	2018, 11, 28,22:59:30	54.39078167	18.57872833	62	7	2.5	325.9	325.9
5	6537591.987	6029105.166	62	2018, 11, 28,22:59:31	54.39079667	18.57874167	62	6	3.1	326	326

Each observation recorded with frequency of 1 Hz and saved as a NMEA 0183 message was converted into a single data line with a unique identifier of measurement data ID_{pom}. The curvilinear geodetic coordinates (latitude and longitude) were converted to the coordinates $x_{PL-2000}$, $y_{PL-2000}$ of the PL-2000 coordinate system. The orthometric height H_{Ort} from the $GPGGA message and the observation time from the $GPZDA was saved in the data record. It also contained the number of

satellites used for the compass positional solution (SVs), HDOP and two course values (HDG$_1$ and HDG$_2$) from the $GPHDT message. The information about the course was placed in the data record twice, as the $GPHDT message does not contain the time identifier. Therefore, an approach was applied which includes the use of the readings for the preceding and following courses relative to the successive messages $GPZDA, $GPGGA and $GPGLL.

The input file for the program, with the reference data from the satellite receiver measurements conducted at the frequency of 20 Hz, had the structure shown in Table 3. Similarly to the file with satellite compass data, each observation for the reference satellite receiver was assigned a unique identifier ID$_{ref}$. A data record consisted of point coordinates in the PL-2000 system ($y_{PL-2000}$, $y_{PL-2000}$) and a normal height (H$_N$) calculated from the ellipsoidal height (h$_{el}$), taking into account the value of undulation interpolated from the geoid model by the GNSS receiver.

Table 3. Fragment of the input file containing satellite receiver reference observations.

ID$_{ref}$	y$_{PL-2000}$ [m]	x$_{PL-2000}$ [m]	H$_N$ [m]	Geoid Undulation [m]	h$_{el}$ [m]
1	6540807.909	6031163.238	2.2104	29.3426	31.553
2	6540807.91	6031163.239	2.215	29.3426	31.5576
3	6540807.909	6031163.24	2.2114	29.3426	31.554
4	6540807.91	6031163.24	2.2164	29.3426	31.559
5	6540807.909	6031163.24	2.2124	29.3426	31.555

Determination of the satellite compass positioning error involved projecting the point determined by the satellite compass onto a curve made up by the reference observations (further referred to as the track axis to make the description simpler). Since the deviations of the points from the track were relatively small, no approximation of the local curve course was made and a simplified approach was used which involved identification of the nearest point from the reference set and determination of the distance between two points. The problem was solved by applying two hierarchically placed loops. The first loop fed consecutive records from the satellite compass file. For each iteration, the program performed another loop, which fed the reference file and sought the optimum point (marked ref) according to the criterion of the smallest distance to the point in question determined by the satellite compass (marked P). After assigning the nearest reference point ref to the point P under examination, the identifiers ID$_{pom}$ and ID$_{ref}$ values were written in the respective variables. A linear error of an individual satellite compass observation was the distance:

$$m_d = \sqrt{\left(x_P - x_{ref}\right)^2 + \left(y_P - y_{ref}\right)^2}$$ (2)

where:

m_d—positioning linear error,
x_P, y_P—rectangular coordinates of the point measured by the satellite compass,
x_{ref}, y_{ref}—rectangular coordinates of the reference point measured by the satellite receiver.

Error calculation for the course determination by the satellite compass was performed by comparing the value determined by the device with the azimuth of the tangent to the track axis at the reference point. Having a record identifier ID$_{ref}$ from the reference file, the software was able to create a subordinate set of reference points based on which the line parameters and the azimuth were defined. A limit radius length of 0.5 m was applied. Considering the mean distance between reference points of 0.20 m, the adopted radius length ensured there was a sufficient sample size, which provided the basis for approximation of the tangent to the tramway track curve by using the least squares method. The known parameters of the tangent (the slope) can be used to determine the line azimuth, which is further used as the comparative reference value for the course saved in the $GPHDT message. The diagram of selection and approximation is shown in Figure 6.
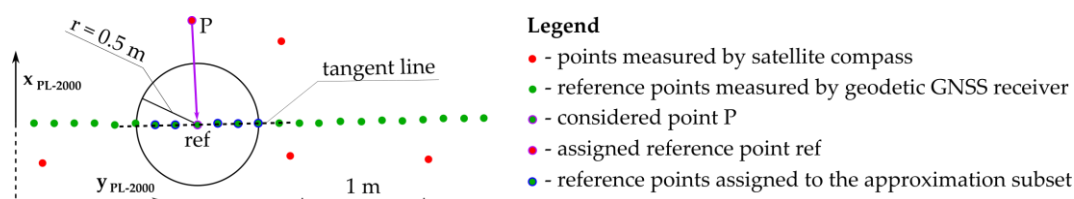
Figure 6. The determination diagram for the track tangent parameters at point P.

The tangent parameters (slope and intercept) were determined with the polyfit function of the SciPy Python library. The function fits a polynomial of the predefined degree into a set of points. In the case in point, it is a straight line, so it is a first degree polynomial. Therefore, the Vandermonde matrix used in the estimation [29] is a two-column matrix. The error minimisation is the alignment criterion [30]:

$$E = \sum_{j=0}^{k} \left| p(x_j) - y_j \right|^2 \tag{3}$$

where:

E—error (linear distance of a point from the straight line being estimated),
p—Vandermonde matrix,
x_j, y_j—rectangular coordinates of the points being fitted in (here: PL-2000 system coordinates).

The polyfit function returns the slope value and the intercept. According to the definition, the slope is the tangent of the left-hand angle between a line and the OX axis of the mathematical coordinate system [31]. The accuracy of the course parameter determined by the satellite compass and the azimuth are right-hand angles counted from the northward direction (the OY axis in the mathematical coordinate system). Additionally, the relative position of the start and end point of the line is important for the azimuth. In order to determine the azimuth at a given track axis point, it is necessary to introduce conditions for coordinates increments of the extreme points of a reference sample and to recalculate the slope value accordingly (4). The conditional formula retains the mathematical axes arrangement—OX eastwards, OY northwards.

$$Az = \begin{cases} \arctan\left(\frac{1}{a_{st}}\right) & (dy \geq 0) \wedge (dx \geq 0) \\ \frac{\pi}{2} & (dy = 0) \wedge (dx > 0) \\ \arctan\left(\frac{1}{a_{st}}\right) + \pi & dy < 0 \\ \frac{3\pi}{2} & (dy = 0) \wedge (dx < 0) \\ \arctan\left(\frac{1}{a_{st}}\right) + 2\pi & (dy > 0) \wedge (dx < 0) \\ undefined & (dy = 0) \wedge (dx = 0) \end{cases} \tag{4}$$

where:

Az—azimuth of the tramway track axis at point P under examination,
a_{st}—slope of the track axis tangent,
dx—increment of eastern rectangular coordinates of the PL-2000 system ($y_{PL-2000}$),
dy—increment of northern rectangular coordinates of the PL-2000 system ($x_{PL-2000}$),

The curvilinear shape of projected meridians in the Gauss-Krüger projection and in the PL-2000 coordinate system should be taken into account in determination of the real azimuth of the tramway track axis. Therefore, the azimuth value calculated with formula (4) must be adjusted to include the effect of convergence [28]. Elimination of the convergence effect involves taking into account the negative value of the direction angle of a meridian (or the OX axis of the conventional primary system) in the projectional plane system (secondary). The effect of convergence is shown in Figure 7.

The correction for the direction reduction was omitted because of the very small distances between the extreme points of reference point subsets.
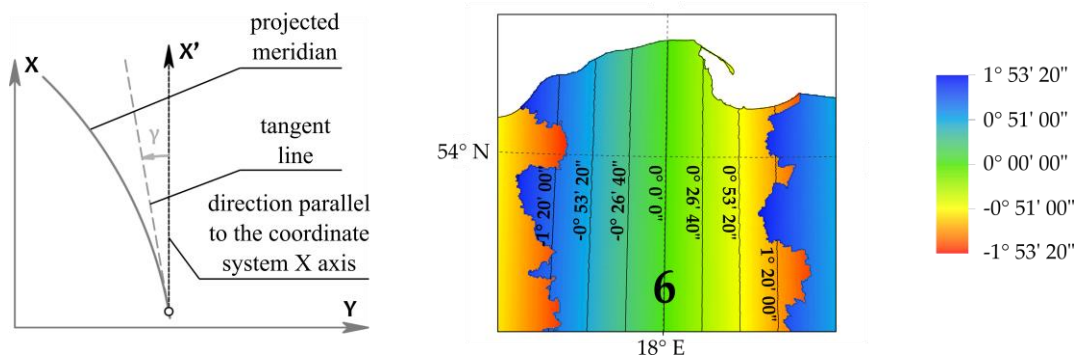
Figure 7. Convergence of the meridian projection in the PL-2000 coordinate system and its values for the area of Pomeranian Voivodship.

Convergence depends both on the geodetic latitude and longitude and it is calculated with the formula [32]:

$$\gamma = l \cdot \sin(B) + \frac{l^3}{3}\sin(B) \cdot \cos^2(B) \cdot \left(1 + 3(e\prime\cos(B))^2\right) + \frac{l^5}{15}\sin(B) \cdot \cos^4(B) \cdot \left(2 - tg^2(B)\right) \quad (5)$$

where:

γ—convergence,

l—difference between the geographic longitude of the point and the geographic longitude of the zone axial meridian,

B—geodetic latitude of point P under examination,

$e\prime$—second eccentricity of GRS80 ellipsoid.

Considering the small analysis area, the convergence was calculated for the area centre of gravity and the value of $\gamma = 0.51°$ was obtained, which was adopted as the constant value for the whole study area. Knowing the reference value of azimuth Az and convergence γ, one can compare it with the course HDG saved in the $GPHDT message and determine the error of course determination by using the satellite compass:

$$m_{HDG} = HDG - (Az + \gamma). \quad (6)$$

Having the values of height determined by the satellite compass (H_{Ort}) and by using the reference satellite receiver (H_N), the height error (m_H) could be determined. A simplifying assumption was made which involved comparing the normal height and the orthometric height due to the assumption of a large similarity of the geoid and the quasigeoid in the area under analysis.

$$m_H = H_{Ort} - H_N \quad (7)$$

The last operation in the secondary loop was used to save the results in the output text file with the structure presented in Table 4. Each record of the file data was marked with an identifier (ID_{pom}) and flat coordinates ($x_{PL-2000}$, $y_{PL-2000}$) of the point measured by the satellite compass. Further columns contain the calculated height error (m_H), number of satellites used in the positioning solution (SVs), HDOP, the positioning linear error (m_d), calculated reference azimuth of the tangent to the track axis (Az), registered course value (HDG) and the error of course determination with its absolute value (m_{HDG}, $|m_{HDG}|$).

Table 4. Fragment of the output file containing calculation results.

ID_{pom}	$y_{PL-2000}$ [m]	$x_{PL-2000}$ [m]	m_H [m]	SVs [−]	HDOP [−]	m_d [m]	Az [°]	HDG [°]	m_{HDG} [°]	$|m_{HDG}|$ [°]
4018	6540650.569	6031030.820	36.99	9	1.5	0.56	188.36	189.5	0.63	0.63
4019	6540650.265	6031028.591	35.99	8	1.8	0.55	187.71	189.7	1.48	1.48
4020	6540650.168	6031027.292	35.99	8	1.8	0.61	187.02	190	2.47	2.47
4021	6540649.758	6031024.691	35.99	8	1.8	0.50	186.15	190.2	3.54	3.54
4022	6540649.455	6031022.276	35.99	8	1.8	0.46	186.49	190.5	3.50	3.50

A total of 2039 records were obtained and taken for the final conclusions from the study. A statistical error analysis for the position, course, and height determination was conducted based on the sample and the results are provided in the next chapter of the paper.

3. Results and Discussion

Errors of positioning by the Furuno SC-50 satellite compass of the relative reference route measured by the geodetic satellite receiver by the RTK differential method are shown in Figure 8. The greatest positioning errors occurred in the last section of the test route loop which runs among buildings close to the track (Figure 2), where values approaching 7.5 m were recorded. The error in a great majority of position determinations was not larger than 1 m (see the histogram on the right of the legend to Figure 8). There were sections with higher errors in some parts of the north-eastward test route. It is noteworthy that there were roadside trees and buildings in this section. One can also observe that the positioning error with a compass can increase locally when the tramway changes directions on bends. This may be caused by the Kalman filter algorithm, which is widely used in devices used for navigation and positioning.
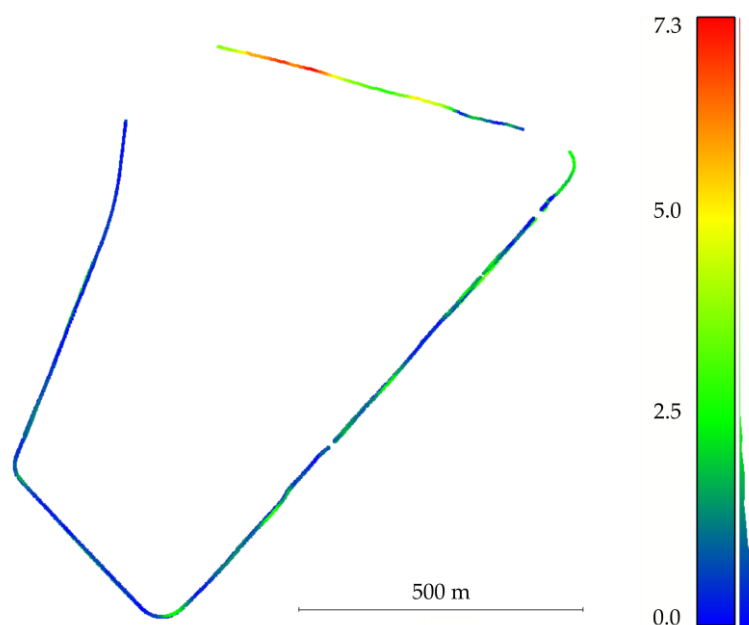
Figure 8. Error of horizontal positioning with a satellite compass m_d [m].

A listing of the number of observations with specific errors and the basic statistical data for a sample is shown in Figure 9.

Statistical measure [m]	
Arithmetic average	1.10
Standard deviation	1.15
Median	0.76
Minimum	0.01
Maximum	7.34
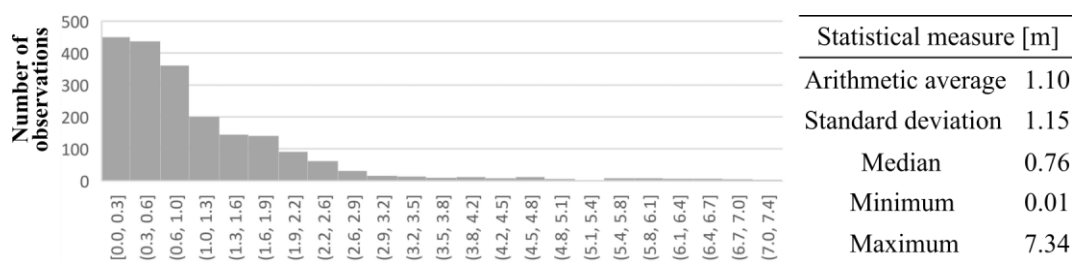
Figure 9. A histogram of error distribution for horizontal positioning by the satellite compass with the sample statistical parameters.

The error distribution for the course of the device under study is shown in Figure 10. The majority of the observations did not exceed an error of 10°. The errors were similar in the test sections, along which there were no sudden changes of direction. It must be stressed that the greatest course errors, which occurred along Gdańska Street (Figure 2), were smaller in the other tramway passages. Considering that worse accuracy parameters were maintained nearly throughout the whole straight-line section, this may suggest that they can be attributed to an unfavourable constellation of the GPS satellites. The histogram and the basic statistical data for the sample are shown in Figure 11.
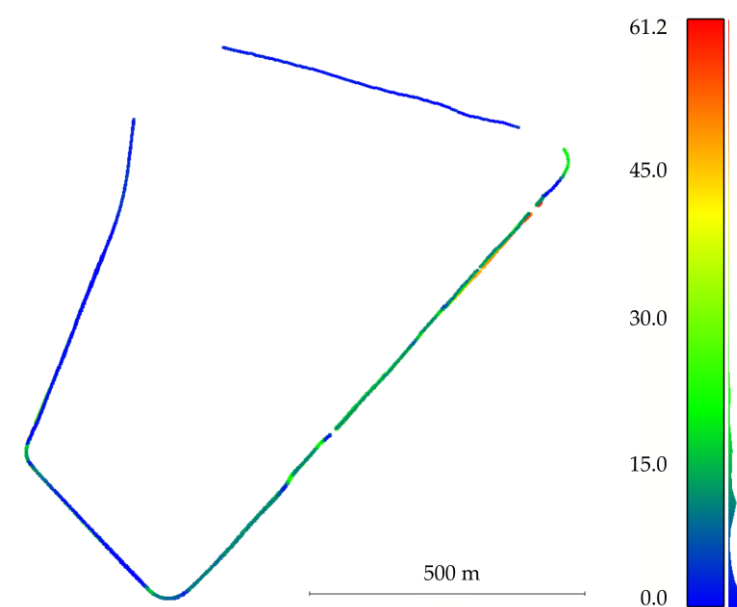
Figure 10. The course determination error by the satellite compass m_{HDG} [°].

Statistical measure [°]	
Arithmetic average	12.72
Standard deviation	13.02
Median	10.48
Minimum	0.00
Maximum	61.23
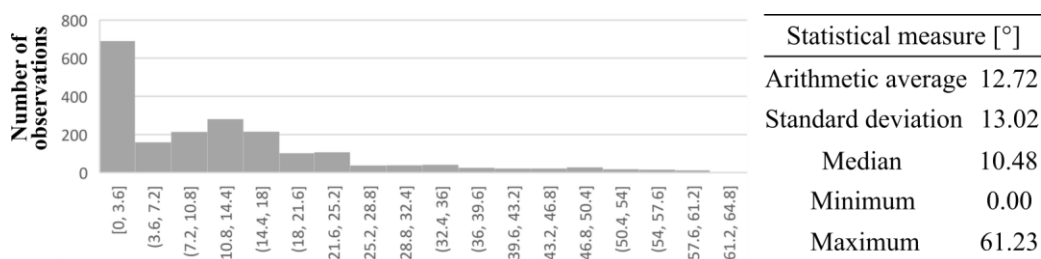
Figure 11. A histogram of error distribution course determination by the satellite compass with the sample statistical parameters.

Due to the significant exceeding of the course accuracy threshold value provided by the compass manufacturer, an additional analysis was carried out to confirm the obtained result. The check consisted of two independent calculations. The first control analysis used the algorithm presented with the

formulas (3)–(6), with the difference that the determination of the slope coefficient a_{st} in the estimation (3) was based on a radius r = 1.0 m (instead of previous radius of 0.5 m) to detect potential negative impact of too few reference points on determining the parameters of the line tangent to the axis of the tram track. A histogram of the course error values obtained for the radius r = 1.0 m and statistical parameters of the sample are presented in Figure 12. The result of the analysis confirmed the correctness of the previous determination by obtaining similar results.

Statistical measure [°]	
Arithmetic average	12.72
Standard deviation	13.05
Median	10.53
Minimum	0.00
Maximum	59.60
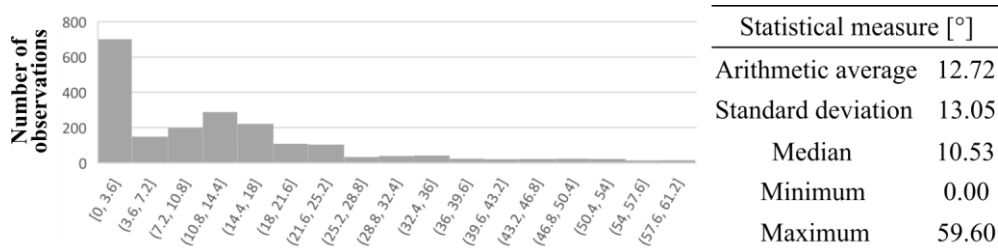
Figure 12. A histogram of error distribution course determination by the satellite compass with the sample statistical parameters in control analysis.

The second stage of the control analysis consisted in comparing the satellite compass course readings on 11 straight sections of the route. Geometric parameters of straight sections were obtained by fitting a straight line into a set of two-dimensional points by using the least squares method [12]. Within each of the control sections, the azimuth value was determined, which was compared with the average azimuth calculated in accordance with the algorithm (3)–(4) for the compass observations along the reference line. The location of rectilinear control sections is shown in Figure 13.
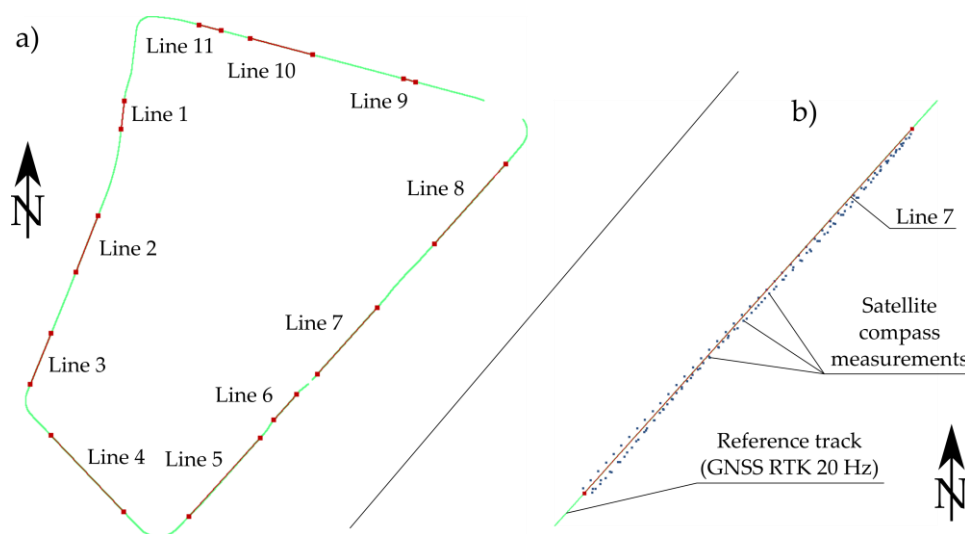
Figure 13. Eleven rectilinear control sections of the tram track axis (**a**) with detailed view of one of the lines (**b**).

The results of the second control analysis are presented in Table 5. The column "Line azimuth" contains the value of azimuths of the straight line test sections. The "Estimated azimuth" column shows the corresponding average azimuth value obtained in the controlled analysis (Figure 10) limited to the compass readings recorded along the tested line (Figure 13b). Again, the results confirmed the correctness of the results obtained in the first calculation. The average azimuth values obtained by the estimation presented in the formula (3) do not differ by more than 0.06° from the corresponding azimuth values that are appropriate for straight sections of the tram track. Therefore, when comparing the error values of the compass heading (Figure 11) with the above azimuth deviation of 0.06°, it is legitimate to assume that the error values obtained were determined correctly.

Table 5. Results of the second control analysis of the azimuth value.

Line		Easting [m]	Northing [m]	dEast [m]	dNorth [m]	Distance [m]	Line Azimuth [°]	Estimated Azimuth [°]	Azimuths Difference [°]
Line 1	start	6540648.490	6031017.935	−6.286	−54.874	55.233	186.53	186.53	−0.01
	end	6540642.204	6030963.061						
Line 2	start	6540597.046	6030792.950	−43.114	−109.869	118.025	201.43	201.44	0.01
	end	6540553.932	6030683.081						
Line 3	start	6540505.546	6030562.915	−40.746	−99.843	107.837	202.20	202.20	0.00
	end	6540464.800	6030463.072						
Line 4	start	6540504.876	6030362.904	142.684	−149.854	206.918	136.40	136.41	0.01
	end	6540647.560	6030213.050						
Line 5	start	6540774.045	6030203.881	139.905	154.252	208.248	42.21	42.16	−0.05
	end	6540913.950	6030358.133						
Line 6	start	6540940.432	6030393.111	44.540	49.786	66.802	41.82	41.82	0.00
	end	6540984.972	6030442.897						
Line 7	start	6541025.520	6030483.008	116.591	129.894	174.545	41.91	41.93	0.02
	end	6541142.111	6030612.902						
Line 8	start	6541254.036	6030738.005	139.942	156.789	210.158	41.75	41.69	−0.06
	end	6541393.978	6030894.794						
Line 9	start	6541217.262	6031055.092	−23.137	6.127	23.935	284.83	284.84	0.01
	end	6541194.125	6031061.219						
Line 10	start	6541015.911	6031108.283	−121.830	32.175	126.007	284.79	284.74	−0.05
	end	6540894.081	6031140.458						
Line 11	start	6540837.631	6031155.385	−43.590	11.492	45.079	284.77	284.77	0.00
	end	6540794.041	6031166.877						

These course determination errors are absolute values of leftward or rightward tilts relative to the current journey direction. Figure 14 contains information on the errors broken down into two sides: left (negative) and right (positive). Considering the study which is the subject of this paper (a specified test route, variable directions, and length of partial sections), the results are a special case and it would not be justified to draw general conclusions. However, it is interesting that there is a majority of positive errors for course determination with a satellite compass.
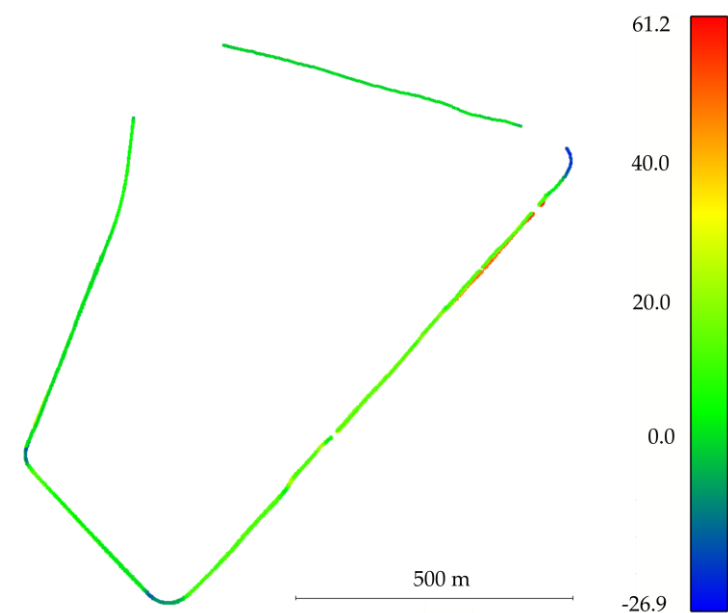

Figure 14. The error of course determination by a satellite compass m_{HDG} [°], with the orientation relative to the direction of the tramway journey.

Switching from the horizontal to the vertical dimension, the following is a result of accuracy analysis for height determination by the device under study (Figure 15). All errors, except for the 1 cm deviations from full metres, exceed 27 m and reach 51 m. More detailed statistical data are presented next to the histogram (Figure 16).
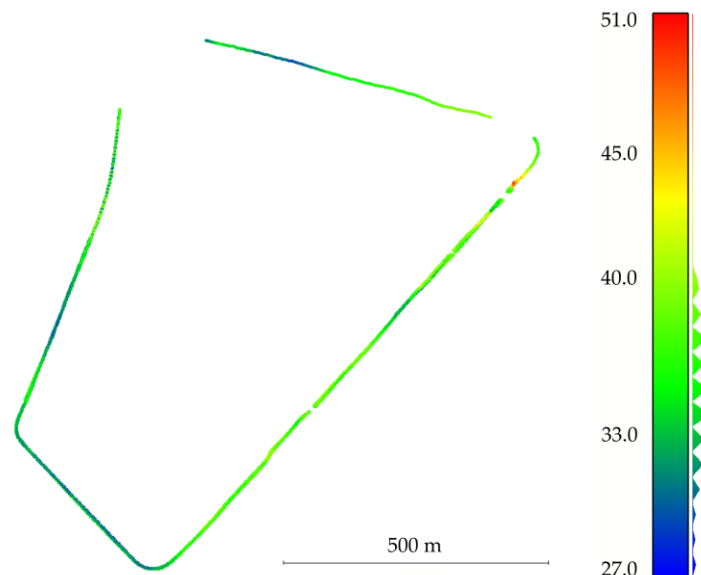
Figure 15. The error of height determination by the satellite compass m_H [m].

Statistical measure [m]	
Arithmetic average	34.79
Standard deviation	3.38
Median	34.99
Minimum	26.99
Maximum	50.99
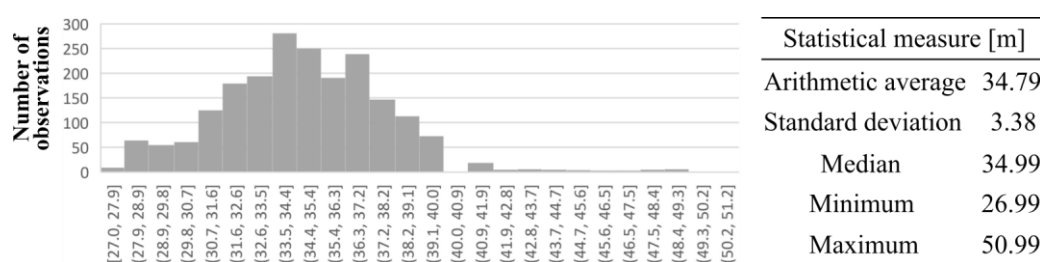
Figure 16. A histogram of error distribution for height determination by the satellite compass with the sample statistical parameters.

Relatively small standard deviations for the data indicate that there is a constant systematic error in all the observations. According to the author, the ellipsoid height may not have been converted to orthometric or normal height. The distance between the geoid and the ellipsoid of revolution WGS84 in the area under study would be about 29.35 m (Table 3). After the correction is taken into account, the determination errors would be much smaller, which indicates a potential cause of low accuracy.

The GPS satellite constellation changed during the nearly two-hour measurement. Its distribution is demonstrated by the number of available satellites and the HDOP. The first parameter is shown in Figure 17. The histogram was presented in Figure 18. In the majority of cases, the satellite compass received a signal from seven satellites, although also slightly less frequently from six or eight satellites. The highest values of this parameter were recorded in sections with a small number of trees or buildings obscuring the satellite signal (Józef Haller Avenue and Maciej Płażyński Avenue). Four is the minimum number of available satellites, which—according to the literature—is the necessary condition for positioning.
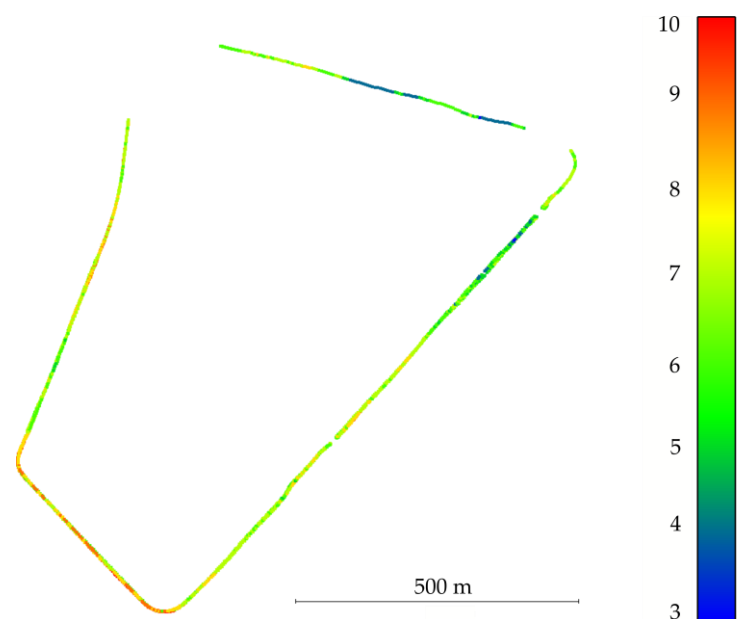
Figure 17. The number of available satellites observed by the satellite compass on the test route.
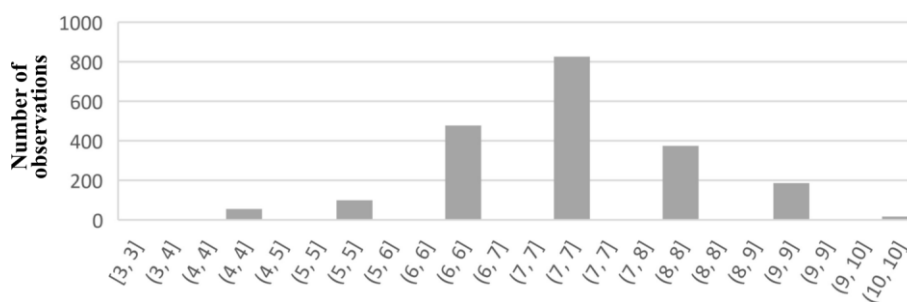
Figure 18. A distribution histogram for the number of available satellites.

The final analysis concerned the HDOP. The distribution of the parameter values is shown in Figure 19. A detailed histogram is shown in Figure 20. The mean for the sample is 2.25 with a standard deviation of 0.080, which indicates that there were favourable conditions regarding the geometric satellite constellation for conducting measurements in the area. The highest values of the HDOP index were calculated for the northern section of the test route running through densely built-up areas.

The results proved that the device partially fulfilled the producer's specification regarding the device accuracy in the measurement conditions. The positioning error did not exceed 7.5 m, with the vast majority of errors below 1.5 m. The positioning error without DGPS corrections was 10 m. The compass height error ranged from 27 to 51 m. Such a large error may indicate that the geoid model was not used in height determination. The course error did not exceed 10.5° in half of the measurements, with the largest error set containing values ranging from 0 to 3.6°. These values exceeded the level of 0.5° declared in the specification. However, one should take into account more difficult measurement conditions than the standard conditions at sea and full visibility of the sky.

Figure 19. The HDOP geometric index along the test route.

Figure 20. A histogram of the HDOP with the sample statistical parameters.

4. Conclusions

Test measurements of the Furuno SC-50 satellite compass were conducted at night on 28/29 November as part of the measurement campaign conducted as part of the InnoSatTrack research project. An atypical device working environment—an urban setting—was a signi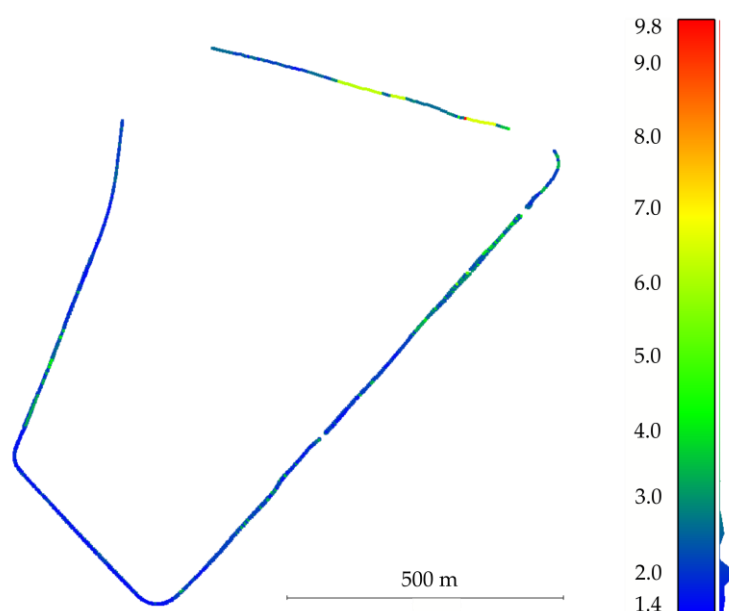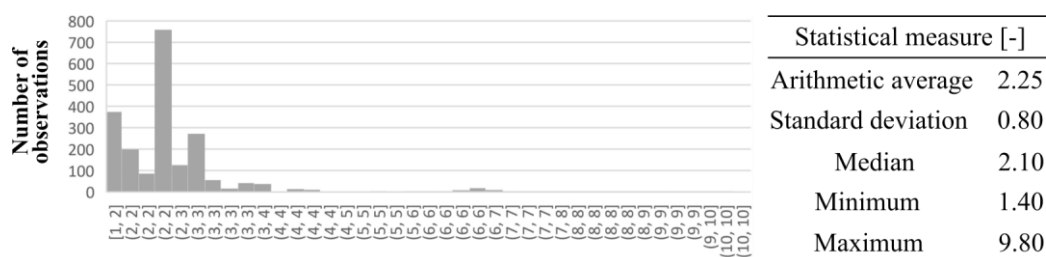ficant feature of the experiment. The measurements were conducted on a tramway track in Gdańsk Brzeźno. The route was a closed loop consisting of four sections of various degrees of sky visibility (due to the presence of, for example, trees and buildings). The objective of the experiment was to empirically determine the error of positioning and course determination with a satellite compass. The results were compared to a reference route measured with a precision two-frequency receiver operating in the GNSS RTK differential mode, ensuring centimetre accuracy for determining individual points on the track axis. The proposed methodology included an evaluation of positioning accuracy based on the distance to the nearest points of the reference route. The course determination by a compass was evaluated by approximation by the least squares method of the parameters of the track axis tangent at the assigned reference point. The authors for this study developed software in the Python language; the program used input files with observations of the compass under study and the reference receiver. The Furuno SC-50 ensures reliable determination of the horizontal position in an urban setting (mean error of 1.5 m). The altitude coordinate has a considerable systematic error of several dozen meters. The course indicated by the device in the urban environment exceeds the values specified by the producer by several-fold.

Author Contributions: Conceptualization, P.S.D. and A.F.; methodology, P.S.D., A.F.; software, P.S.D.; validation, P.S.D. and A.F.; formal analysis, C.S. and A.F.; resources, K.J., C.S., W.K., A.W., K.C., K.K., P.C., M.S. and J.S.;

References

1. GPS Standard Positioning Service (SPS) Performance Standard, 4th ed. Available online: http://www.gps.gov/technical/ps/ (accessed on 10 August 2019).

2. Misra, P.; Enge, P. *Global Positioning System: Signals, Measurements and Performance*, 2nd ed.; Ganga-Jamuna Press: Lincoln, OR, USA, 2012.

3. Specht, C.; Dąbrowski, P. Runaway PRN11 GPS satellite. In Proceedings of the 10th International Conference "Environmental Engineering", Vilnus, Lithuania, 27–28 April 2017. [CrossRef]

4. Teunissen, P.; Montenbruck, O. *Springer Handbook of Global Navigation Satellite Systems*; Springer: Cham, Switzerland, 2017.

5. Specht, C.; Dabrowski, P.S.; Pawelski, J.; Specht, M.; Szot, T. Comparative analysis of positioning accuracy of GNSS receivers of Samsung Galaxy smartphones in marine dynamic measurements. *Adv. Space Res.* **2019**, *63*, 3018–3028. [CrossRef]

6. Furuno Manual, THD Satellite Compass, Model SC-50. Furuno Electric Co., LTD. Available online: http://www.furuno.se/fileadmin/files/Manuals/6_Pilot_Comp/SC-50/SC-50_OM_ENG_72510F.pdf (accessed on 10 August 2019).

7. Specht, C.; Nowak, A.; Koc, W.; Jurkowska, A. Application of the Polish Active Geodetic Network for railway track determination. In *Transport Systems and Processes: Marine Navigation and Safety of Sea Transportation*; Weintrit, A., Neumann, T., Eds.; CRC Press: Boca Raton, FL, USA, 2011; pp. 77–81.

8. Specht, C.; Mania, M.; Skóra, M.; Specht, M. Accuracy of the GPS Positioning System in the Context of Increasing the Number of Satellites in the Constellation. *Pol. Marit. Res.* **2015**, *22*, 9–14. [CrossRef]

9. Specht, C.; Specht, M.; Dąbrowski, P. Comparative Analysis of Active Geodetic Networks in Poland. In Proceedings of the 17th International Multidisciplinary Scientific GeoConference SGEM 2017, Albena, Bulgaria, 29 June–5 July 2017. [CrossRef]

10. Specht, C.; Koc, W.; Smolarek, L.; Grządziela, A.; Szmagliński, J.; Specht, M. Diagnostics of the Tram Track Shape with the use of the Global Positioning Satellite Systems (GPS/Glonass) Measurements with a 20 Hz Frequency Sampling. *J. Vibroeng.* **2014**, *16*, 3076–3085.

11. Specht, C.; Koc, W. Mobile Satellite Measurements in Designing and Exploitation of Rail Roads. *Transp. Res. Proc.* **2016**, *14*, 625–634. [CrossRef]

12. Specht, C.; Koc, W.; Chrostowski, P.; Szmaglinski, J. Accuracy Assessment of Mobile Satellite Measurements Relation to the Geometrical Layout of Rail Tracks. *Metrol. Meas. Syst.* **2019**, *26*, 309–321. [CrossRef]

13. Koc, W. Design of Rail-Track Geometric Systems by Satellite Measurement. *J. Transp. Eng.* **2012**, *138*, 114–122. [CrossRef]

14. Koc, W. The analytical design method of railway route's main directions intersection area. *Open Eng.* **2016**, *6*, 1–9. [CrossRef]

15. Koc, W.; Specht, C.; Chrostowski, P.; Szmagliński, J. Analysis of the possibilities in railways shape assessing using GNSS mobile measurements. In Proceedings of the MATEC Web Conf. Scientific Conference of the Committee for Civil Engineering of the Polish Academy of Sciences and the Science Committee of the Polish Association of Civil Engineers (PZITB), Krynica, Poland, 16–20 September 2018. [CrossRef]

16. Specht, C.; Chrostowski, P.; Koc, W. Computer-aided evaluation of the railway track geometry on the basis of satellite measurements. *Open Eng.* **2016**, *6*, 125–134. [CrossRef]

17. Lu, G.; Cannon, M.E.; Lachapelle, G.; Kielland, P. Attitude determination in a survey launch using multi-antenna GPS technologies. In Proceedings of the National Technical Meeting, the Institute of Navigation, Alexandria, VA, USA, 20 January 1993.

18. Comp, C.J. Optimal antenna configuration for GPS based attitude determination. In Proceedings of the ION GPS-93, Salt Lake City, UT, USA, 22–24 September 1993; pp. 773–779.

19. Ueno, M.; Santerre, R.; Babineau, S. Impact of Antenna Configuration on GPS Attitude Determination. In Proceedings of the 9th World Congress of International Association of Institutes of Navigation (IAIN'97), Amsterdam, The Netherlands, 20 November 1997.

20. Felski, A.; Mięsikowski, M. Some Aspects of DGPS Based Heading Determination. *Geodezja i Kartografia* **1999**, *48*, 97–104. (In Polish)

21. Felski, A. Exploitative properties of different types of satellite compasses. *Annu. Navig.* **2010**, *16*, 33–40.

22. Jaskólski, K.; Felski, A.; Piskur, P. The Compass Error Comparison of an Onboard Standard Gyrocompass, Fiber-Optic Gyrocompass (FOG) and Satellite Compass. *Sensors* **2019**, *19*, 1942. [CrossRef] [PubMed]

23. Feng, Y.; Wang, J. GPS RTK performance characteristics and analysis. *J. Glob. Position. Syst.* **2008**, *7*, 1–8. [CrossRef]

24. Regulation of the Council of Ministers of October 15, 2012 on the state system of spatial references (Dz.U. 2012 poz. 1247). 2012. (In Polish)

25. Wilk, A.; Specht, C.; Koc, W.; Karwowski, K.; Chrostowski, P.; Szmagliński, J.; Dąbrowski, P.; Specht, M.; Judek, S.; Skibicki, J.; et al. Projekt badawczy BRIK: Opracowanie innowacyjnej metody wyznaczania precyzyjnej trajektorii pojazdu szynowego. *Przegląd Komunikacyjny* **2019**, *7*, 18–27. (In Polish)

26. Wilk, A.; Koc, W.; Specht, C.; Karwowski, K.; Chrostowski, P.; Szmagliński, J.; Dąbrowski, P.; Specht, M. Wyznaczanie osi toru i trajektorii pociągu w projekcie BRIK. In Proceedings of the Konferencja "Nowoczesne technologie w realizacji projektów inwestycyjnych transportu kolejowego", Jurata, Poland, 24–26 April 2019. (In Polish).

27. Langley, R.B. NMEA 0183: A GPS receiver interface standard. *GPS World* **1995**, *6*, 54–57.

28. Gajderowicz, I. *Odwzorowania kartograficzne: Podstawy*; Wydawnictwo Uniwersytetu Warmińsko-Mazurskiego w Olsztynie: Olsztyn, Poland, 2009. (In Polish)

29. Hazewinkel, M. *Encyclopaedia of Mathematics: Volume 9 Sto-Zyg*; Kluwer Academic Publishers: Dordrecht, The Netherlands, 1993.

30. Numpy and Scipy Documentation of Site. Available online: https://docs.scipy.org/doc/numpy/reference/generated/numpy.polyfit.html (accessed on 10 August 2019).

31. Bronshtein, I.N.; Semendyayev, K.A.; Musiol, G.; Mühlig, M. *Handbook of Mathematics*, 6th ed.; Springer Science & Business Media: Berlin, Germany, 2015.

32. Kadaj, R. *Technical Regulations G-1.10 Mapping Formulas and Coordinate System Parameters*; Chief Land Surveyor: Warsaw, Poland, 2001. (In Polish)